Applying the Hypercomplex Model to Macromolecules, Catalysis and Metabolism

Richard L. Lewis, PhD, AuG
Independent Researcher

In Papers 1–4, we applied our hypercomplex mathematical model to the spacetime metric, the particle/wavefunction duality, and the structure of atoms and their configurations as molecules. In this fifth paper, we advance from the domains of pure physics and foundational chemistry to examine the very structural underpinnings of biological systems: biochemistry.

I. Introduction: The Topology of Complementarity

In the first four papers of this series, we demonstrated how independent, volatile hypercomplex systems form stable, steady-state structures when paired with their exact algebraic complements. We explored two primary modalities of this framework: its application as a descriptive tool for structural modeling, and its potential role as a foundational aspect of universal quantum laws and the principles of biochemistry. (As a conceptual baseline: any law incorporating an imaginary component may be considered culturally quantum.)

Whatever the precise nature of these quantum laws, they enforce a rigorous structural distinction between left- and right-handed states. To establish a standardized nomenclature, the scientific community utilizes the Latin descriptors dextro (D-, right) and levo (L-, left) to categorize these distinct orientations of identical molecular formulas (see Fig. 1).

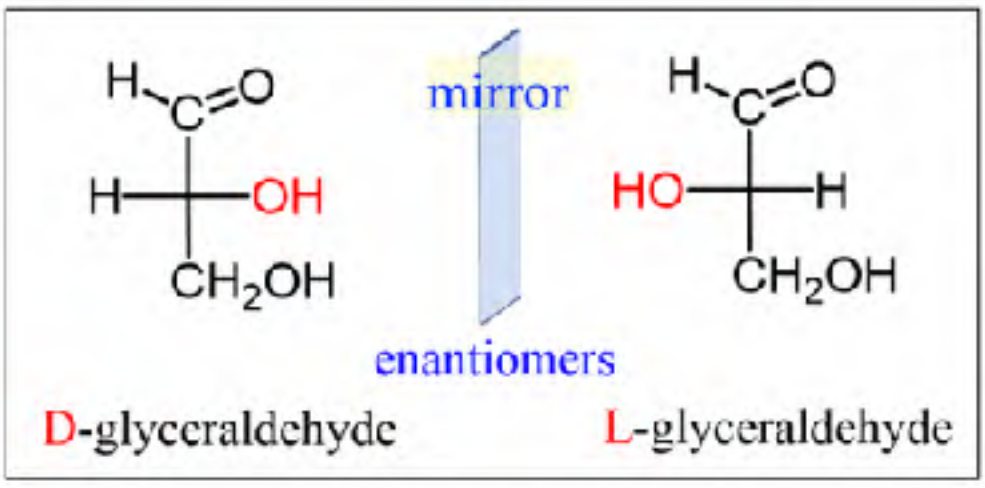

Fig. 1. Stereoisomerism in a simple sugar

For a physicist, this distinction manifests primarily as the differential rotation of polarized light beams. For a synthetic chemist, these differences emerge only when the molecule interacts with another asymmetric or isomeric compound. Within biological systems, however, this spatial distinction is absolute. The D-enantiomer forms the vital metabolic bedrock of terrestrial carbohydrates, whereas its L-counterpart confuses cellular machinery so fundamentally that it is currently being investigated for anti-cancer properties.

These profound functional divergences map directly onto the hypercomplex mathematics of non-associative octonions used to model these molecular spaces.

2. Chirality and Stereochemistry: The 8D Rotational Engine

To formalize why biological systems treat mirror-image enantiomers not as equivalent geometric reflections but as radically distinct functional states, we must elevate our spatial model from the 4D associative quaternionic domain to the 8D non-associative octonionic domain.

An octonion x is expressed over an orthonormal basis:

$$\{e_0, e_1, e_2, e_3, e_4, e_5, e_6, e_7\}$$

where $e_0 = 1$ is the scalar element and $e_1 \ldots e_7$ represent the seven imaginary roots satisfying:

$$e_i^2 = -1 \quad \text{for } i = 1,\ldots,7$$

The multiplication of these imaginary units is dictated by the anti-commutative structural constants:

$$e_i e_j = -\delta_{ij} e_0 + \sum_{k=1}^{7} f_{ijk} e_k$$

The Non-Associative Associator as an Asymmetry Metric

While 3D spatial rotations modeled by quaternions preserve orientation through associative nested actions, the octonionic engine introduces the associator as a non-zero invariant: f_{ijk}

$$e_i e_j = -\delta_{ij} e_0 + \sum_{k=1}^{7} f_{ijk} e_k$$

2.1. The Non-Associative Associator as an Asymmetry Metric

associative nested actions, the octonionic engine introduces the associator as a non-zero invariant:

$$[a, b, c] = (ab)c - a(bc) \neq 0 \quad \forall a, b, c \in \mathbb{O}$$

Because the algebra is alternative, the associator is totally antisymmetric, changing its sign under any permutation of its components. This algebraic property serves as our mathematical definition of structural chirality.

2.2. Chiral Symmetries in Carbohydrates: Spatial Parity Over imaginary Bases

The absolute metabolic preference for D-enantiomers in terrestrial carbohydrate networks implies that biological spaces operate under rigid, high-dimensional parity constraints. To model how a standard monosaccharide ring interfaces with the background biological field, we map its atomic configuration as an internal vector coordinate system.

When a carbohydrate molecule transitions into an aqueous solution, its spatial orientation is not an arbitrary mechanical rotation, but a precise alignment across the non-associative imaginary roots. We define the mirror inversion of an enantiomeric state vector as a mapping that satisfies a localized parity transformation:

$$\mathscr{P} \cdot \Psi_{\text{Carbohydrate}}(e_i) = \Psi_{\text{Carbohydrate}}(-e_i) \quad \text{for } i = 1,\ldots,7$$

Because the background field is alternative, reversing the orientation of these imaginary roots breaks the structural coherence of the localized metabolic engine. The cellular machinery processing a D-sugar relies on the forward cyclic path of the underlying Fano plane; injecting an L-sugar effectively acts as a negative torque operator, locking the enzyme-substrate interface and shutting down downstream glycolytic pathways.

2.3. The Octonionic Splitting of D-Glucose and Structural Locking

We formalize the fundamental structural unit of carbohydrate metabolism by treating the six-carbon ring of D-glucose as a localized hypercomplex state vector. The transformation of a linear hexose chain into its stable cyclic pyranose form represents a geometric closure of vector paths, creating a localized multi-axial torsion pocket.

To track this transformation, we define a localized transition operator that maps the nucleophilic addition of the C-5 hydroxyl group to the C-1 carbonyl carbon:

$$T_{\text{Cyclization}} \cdot \mathbf{V}_{\text{Linear}} = \mathbf{V}_{\text{Ring}}(\alpha) \oplus \mathbf{V}_{\text{Ring}}(\beta)$$

This cyclization splits the background field metric into two distinct stereochemical anomalies: the α-anomer and the β-anomer, defined by the relative spatial trajectory of the newly formed C-1 hydroxyl vector.

Because the underlying algebra is non-associative, these two spatial configurations possess radically distinct path-dependencies. This specific algebraic divergence dictates whether the carbohydrate functions as an elastic, open energy repository (starch) or an

impenetrable, rigid structural matrix (cellulose), setting up the macro-scale structural branch points of life.

2.4. Generalization to Alanine

This exact mathematical mapping applies to L-alanine and its D-enantiomer mirror image. In amino acids, the global background field orientation is inverted relative to sugars, creating a complementary systemic balance.

The central chiral carbon of L-alanine aligns perfectly with this inverse framework, establishing L-amino acids as the universal structural building blocks of functional protein matrices.

On a more philosophical note, homochirality in biochemistry appears to be not a chemical accident of the prebiotic soup, but a structural mandate dictated by high-dimensional rotational engines generating quantum probabilities that are unlike classical motions.

3. Macromolecular Bifurcation: Starch vs. Cellulose

To model how two polysaccharides composed of identical glucose monomers exhibit opposite physical properties, we define the individual glucose ring as a localized hypercomplex state vector. Let the n-th monomer unit in the polymer chain be represented as a vector G_n embedded within a localized sub-manifold of our non-associative space.

The structural evolution of the macromolecule is governed by a discrete transition operator T that dictates how the coordinate frame rotates from one monomer unit to the next:

$$G_{n+1} = T \cdot G_n$$

3.1. Starch and the Continuous α–(1→4) Helix

In starch, the α–(1→4) glycosidic linkage acts as a series of repeating, symmetric spatial transformations. We model this using an identity rotation operator T_α that introduces a 0° relative coordinate phase shift between successive glucose units along the primary axis.

However, because the localized background geometry is non-associative, repeating an identical transformation sequentially causes a progressive, uncompensated drift in the non-abelian vector spaces. This mechanical-algebraic drift forces the polymer chain into a continuous, helical coil:

$$T_\alpha = \exp\left(\frac{\theta}{2} e_i e_j\right)$$

Where θ represents the fixed structural folding angle around the imaginary plane defined by $e_i e_j$. The resulting helical structure leaves wide, open spaces in its geometric wake. These low-energy scalar pockets allow ambient water vectors and digestive enzyme active sites to easily penetrate and cleave the polymer chain.

3.2. Cellulose and the Alternating β-(1→4) Linear Inversion

In cellulose, the β-(1→4) glycosidic linkage introduces a fundamentally different geometric constraint. To achieve structural stability, every successive glucose monomer must be flipped 180° relative to its predecessor. We define this alternating transformation using an inversion operator T_β.

$$T_\beta = \exp\left(\frac{\pi}{2} e_k e_l\right)$$

Because $\exp(\frac{\pi}{2} e_k e_l) = e_k e_l$, the transition operator acts as a pure imaginary axis reflection. The structural state vector of the chain fluctuates deterministically between alternating orientations:

$$G_{n+1} = (e_k e_l) \cdot G_n$$

This exact 180° inversion cancels out the non-associative directional drift that occurs in starch. The progressive vector additions remain perfectly straight, flattening the polymer into an unbranched, strictly linear chain.

3.3 Inter-Chain Locking Mechanics

Because the cellulose chains are perfectly linear, they can align perfectly parallel to one another in dense, macroscopic sheets. This tight spatial alignment allows the hypercomplex field operators of adjacent parallel chains to cross-link via dense hydrogen bonding networks:

$$\Psi_{\text{Total}} = \sum_m \langle G_{n,m}, G_{n,m+1} \rangle$$

This dot product maximizes across the entire lattice, tightly binding the parallel sheets together to construct rigid, impenetrable microfibrils. This comprehensive geometric locking mechanism stabilizes the internal scalar energy of the system, making cellulose chemically inert, insoluble, and completely immune to standard human enzymatic cleavage in the gut.

4. Enzymatic Catalysis: The Hypercomplex Geometric Mold

A remarkable attribute of biochemistry is the extensive array of minerals and substrates that the aqueous enzyme complexes of life can transform. While the high evolutionary specialization of complex multicellular organisms often restricts their

metabolic pathways, simple bacteria and archaea possess vast metabolic versatility—including the capacity to metabolize inorganic rock matrices.

Throughout their two-billion-year dominance of Earth, these microorganisms radically altered global geochemistry, culminating in the planetary oxygenation event. Every aspect of this massive biogeochemical processing is driven by protein enzymes utilizing specialized catalytic active sites where the core reactions occur.

4.1. The Active Site as an Algebraic Sink

Classical biochemistry relies heavily on the mechanical "lock-and-key" or "induced fit" paradigms to describe enzymatic pathways. Within our hypercomplex project framework, we redefine the enzyme's active site as a rigid, high-dimensional algebraic sink or a native subspace mold.

Let the unbound substrate molecule be represented as an unconstrained state vector S moving within an open, high-degree-of-freedom non-associative manifold. The active site of the enzyme is modeled as a highly localized, structurally fixed subspace configuration matrix M_E . When the substrate vector encounters this boundary, it is drawn into the localized potential well of the enzyme through an algebraic projection map:

$$P_E(S) = \sum_i \langle S, \phi_i \rangle \phi_i$$

Where ϕ_i represents the orthogonal imaginary basis elements that construct the rigid geometry of the catalytic pocket. This projection map acts as a geometric filter, trapping the substrate's vector components and forcing them into alignment with the inner coordinate frame of the enzyme matrix.

4.2. Mechanical-Algebraic Vector Warping

Once enclosed within the mold matrix M_E, the substrate's internal vector bonds—which dictate its standard geometric confirmation—are subjected to extreme structural forcing. In a simple attack, breaking or rearranging these bonds requires overcoming a steep physical barrier. The enzyme bypasses this by introducing a localized non-associative distortion operator D, which acts directly on the substrate's internal associator:

$$D \cdot [S_1, S_2, S_3] = (M_E S_1)(S_2 S_3) - S_1(S_2(M_E S_3))$$

This distortion operator forces the substrate's internal vector spaces to warp, stretch, and bend. By physically rotating the molecular orbital representations across high-dimensional imaginary axes, the enzyme effectively changes the localized rules of spatial interaction. The chemical bonds are no longer held in their stable, ground-state geometric orientations; instead, they are forced into a state of structural vulnerability.

4.3. Scalar Energy Relaxation and Activation Barrier Lowering

The direct consequence of this hypercomplex vector forcing is the dramatic relaxation of the system's localized scalar energy requirement. We can formalize the activation energy E_A of the reaction as a function of the localized scalar Hamiltonian H_0. Under standard uncatalyzed conditions, the energy barrier is a direct result of the geometric rigidity of the substrate's ground-state configuration:

$$E_A = \mathrm{Tr}\left(H_0 \cdot (S \cdot S^*)\right)$$

Within the enzyme active site, however, the transformation matrix alters the background metric tensor. The spatial transformation maps the standard Euclidean scalar product onto a relaxed, hypercomplex non-associative manifold. This structural shift cancels out localized repulsion vectors and drops the system's overall potential energy signature down to a minimized catalytic state E_C :

$$E_C = \mathrm{Tr}\left(H_0 \cdot P_E(S \cdot S^*)\right) \ll E_A$$

By lowering this scalar threshold, the enzyme acts as a localized spatial transformer. It shifts the computational and energetic burden of the reaction away from thermal kinetic collisions (scalar heat energy) and maps it onto the pristine, structural geometry of the high-dimensional background vacuum state. The target chemical transformation can then proceed near effortlessly at ambient temperatures.

5. Macroscopic Biological Fields & Structural Scaling

While the 8D octonionic engine effectively maps localized molecular mechanics—such as stereochemical chirality and localized enzymatic subspace molds—biological systems cannot be understood purely through isolated molecular collisions. Life scales these discrete algebraic nodes into continuous macroscopic networks.

To bridge this gap, we define a structural scaling invariant where the localized non-associative properties of individual molecules coalesce into continuous, high-dimensional biological fields.

5.1. The Scaling Invariant: From Monomers to Manifolds

While the 8D octonionic engine effectively maps localized molecular mechanics—such as stereochemical chirality and localized enzymatic subspace molds—biological systems cannot be understood purely through isolated molecular collisions. Life scales these discrete algebraic nodes into continuous macroscopic networks.

To bridge this gap, we define a continuous global field vector over an 8D differentiable manifold. We define a structural scaling invariant, which integrates the localized non-associative transitions of discrete macromolecular states across the smooth topological space:

$$\mathcal{I} = \int_{\mathcal{M}} \mathrm{Tr}\Big(\Psi_{\mathrm{Global}}(\mathbf{x}) \odot \sum_{n} \delta(\mathbf{x} - \mathbf{x}_n) G_n \Big) d^8\mathbf{x}$$

Where $G_n$represents the discrete state vector of the n-th monomer, $\odot$ denotes the non-associative octonionic product, and δ is the Dirac delta function mapping localized molecular nodes to continuous spatial field vectors.

This operational framework ensures that macroscopic bio-fields directly inherit the high-dimensional symmetries of their foundational chemical constituents

5.2. The Failure of Quaternionic Rigidity in Macro-Systems

Classical field modeling often relies on 4D quaternionic frameworks ($\mathbb{H}$) to describe spatial rotations, electromagnetic vectors, and rigid-body mechanics. However, when applied to fluid, dynamic macroscopic biological systems, the associative property of quaternions introduces severe mathematical rigidity.

In a complex biological system—such as an open thermodynamic metabolic matrix or a firing neural architecture—subsystems must possess degrees of non-local freedom where structural history and path-dependency matter. The octonionic engine ($\mathbb{O}$) introduces non-associativity, which mathematically translates to an orientation-dependent, fluid field topology where the sequence of field interactions directly modifies the background metric tensor.

5.3. Neural Network Architectures as Non-Associative Manifolds

Rather than treating a neural network as a collection of discrete, linear switches (axons and synapses processing binary steps), we model the entire neural architecture as a continuous trajectory carving its way through a high-dimensional, non-associative manifold.

Synaptic Potentials as Coordinates: Localized electrical fields do not merely trigger threshold switches; they warp the local imaginary basis elements of the background biological field.

$$\tilde{e}_i(\mathbf{x}) = \exp\big(V_{\mathrm{syn}}(\mathbf{x})\big) e_i$$

Information Storage as Geometric Distortion: Memory, consciousness, and continuous signal propagation are modeled as steady-state, stable geometric distortions within a high-dimensional manifold.

$$\mathscr{D}_{\mathrm{Oct}} \Psi_{\mathrm{Neural}} = \lambda \big[\Psi_{\mathrm{Neural}}, \bar{\Psi}_{\mathrm{Neural}}, \Psi_{\mathrm{Neural}} \big]$$

Non-Associative Logic Gates: Because the overarching manifold lacks associativity, a signal path moving from Node $\tilde{e}_i(\mathbf{x}) = \exp\big(V_{\mathrm{syn}}(\mathbf{x})\big) e_i$ yields a fundamentally different topological state than a path moving from

$$A \to B \to C \implies (A \odot B) \odot C \neq A \odot (B \odot C).$$

This algebraic path-dependency mirrors the complex, contextual, and non-linear behavior of organic cognitive systems

6. Early Archean Metabolism: The Prototypic Subspace Sink

To validate our hypercomplex field theory at the dawn of biochemistry, we move away from advanced organic neuro-manifolds and examine the primitive, primordial systems that catalyzed life on the early Archean Earth. Before the evolution of protein-based enzymes, metabolic processes had to rely entirely on inorganic, geochemical coordinate structures to force molecular transitions.

6.1. The Primordial Vector Split: $CO_2 + H_2 \rightarrow CH_2O$:

We model the primordial reduction of carbon dioxide via the acetyl-CoA or Wood-Ljungdahl pathway as the ultimate test case for our hypercomplex field theory. In the micro-porous labyrinths of alkaline hydrothermal vents, early carbon fixation occurred across thin, inorganic iron-sulfur (FeS) mineral membranes. We define the reactant ground states as unconstrained, low-symmetry vectors moving within an open aqueous environment:

$$V_{\text{Reactants}} = V(\text{CO}_2) \oplus V(\text{H}_2)$$

6.2. Proton Gradient Forcing Across the Inorganic Membrane:

Primordial vents maintained a steady-state proton gradient: an acidic, proton-rich ocean (H^+) outside meeting an alkaline, hydroxyl-rich hydrothermal fluid (OH^-) inside. This gradient across the semi-permeable FeS barrier sets up a continuous, macroscopic vector field matrix $E_{\nabla \text{H}^+}$. We model this natural proton-motive force not merely as an electrochemical gradient, but as a directed hypercomplex spatial transformer that applies continuous physical stress to the localized background metric tensor of the mineral lattice:

$$E_{\nabla \text{H}^+} = \nabla \otimes \Psi(\text{H}^+)$$

6.3. The Mineral Cage as a Prototypic Subspace Mold:

The microscopic, semi-conducting pores of the FeS (mackinawite) lattice act as the historical precursors to modern enzyme active sites. This inorganic "mineral cage" functions as a raw, primitive subspace mold M_{FeS}. When a linear CO_2 vector is pulled into the pore, the localized coordinate transformation operator T_{Vent} alters its rotational boundaries. The presence of the proton gradient matrix forces a non-associative distortion that relaxes the stable double bonds of the carbon dioxide, bending its linear vector space:

$$M_{\text{FeS}} \cdot V(CO_2) = V(CO_2)_{\text{Bent}}$$

This structural bending lowers the localized scalar energy threshold. The bent, vulnerable carbon state is immediately accessible to the vector projections of ambient hydrogen atoms, allowing for the effortless generation of formaldehyde or early carbohydrate precursors (CH_2O):

$$\Psi_{\text{Synthesis}} = \langle V(CO_2)_{\text{Bent}}, E_{\nabla H^+} V(H_2) \rangle \rightarrow V(CH_2O)$$

By utilizing the natural, spatial geometry of the proton gradient as a non-associative engine, the earliest metabolic pathways of LUCA were able to bypass the need for organic enzymes entirely. Life essentially began as a steady-state geometric distortion, transforming background planetary vector gradients into structured, complex matter.

7. Iron-sulfur clusters in Fano plane coordinates

Iron-sulfur (Fe-S) complexes are ancient, ubiquitous protein cofactors essential for life's most fundamental processes. Their primary roles include driving electron transfer in photosynthesis and respiration, enabling complex chemical catalysis (e.g., nitrogen fixation), and acting as cellular gas sensors to regulate gene expression

7.1. Topology of the $[Fe_4S_4]$ Cubane Core

Geometric Representation: We define the eight vertices of the iron-sulfur cubane cluster as a split-octonionic configuration mapping four Fe atoms and four S atoms.

We map the scalar element e_0 to the center of mass, and the 7 imaginary roots $e_1 \ldots e_7$ to the internal coordination axes of the inorganic cage.

7.2. Projecting the Fano Triads onto Electron Transfer Pathways

Fano Plane Mapping: We express the index lines of the Fano Plane (123,145,167,246,257,347,356) as directional vectors of resonant quantum tunneling through the cluster.

Anti-Commutative Flow: We demonstrate how electron spin-polarization tracks the cyclic arrow orientation of the Fano vertices, defining a topological current operator:

$$J_{ijk} = f_{ijk} \cdot \langle \Psi_{Fe} | e_k | \Psi_S \rangle$$

7.3. The Metalloenzyme Active Site as a Closed Fano Manifold

7.3.1. Evolutionary Progression: From Mineral Matrix to Peptide Scaffolding

The transition from abiotic geochemical matrices to modern metabolic architectures represents a continuous topological stabilization of energy-harvesting interfaces. In the Hadean deep-sea hydrothermal alkaline vent settings detailed in Section 6, primitive

electron transfer pathways relied upon native, disordered [Fe_4S_4] mineral precipitates embedded within inorganic cavern walls.

These primordial mineral cages lacked structural isolation; they were continuously exposed to thermal gradients, localized pH fluctuations, and chaotic fluidic shear stress. This open thermodynamic boundary condition subjected the underlying multi-axial torsion configurations to continuous metric relaxation.

The emergence of modern ferredoxins marks an evolutionary phase transition where biological systems replaced the variable inorganic mineral matrix with a highly conserved, genetically encoded peptide envelope. This sequence-specific protein fold isolates the cubane core from bulk water, substituting erratic geochemical inputs with precise, sterically constrained amino acid coordinate bonds.

7.3.2. The Invariant Conclusion: Elimination of Non-Associative Metric Drift

The overriding functional pressure on modern metalloenzymes is the preservation of precise, ultra-fast quantum tunneling pathways for electron transport. As derived in Section 3, unconstrained octonionic fields exhibit a non-vanishing associator:

$$[A, B, C] \neq 0 \implies g_{\mu\nu}(\mathbf{x}) = \eta_{\mu\nu} + \kappa \cdot \Omega_{\mu\nu\rho} \nabla^{\rho} [\Psi_1, \Psi_2, \Psi_3]$$

8. Sedenion transition parameter framework

8.1. The Direct Algebraic Inversion of Zero

The ultimate justification for upgrading from the 8-dimensional octonionic domain ($\mathbb{O}$) to the 16-dimensional sedenionic domain ($\mathbb{S}$) lies in the emergence of zero divisors.

In all lower-dimensional normed division algebras ($\mathbb{R}, \mathbb{C}, \mathbb{H}, \mathbb{O}$), the product of two non-zero elements is strictly non-zero. The sedenions break this paradigm via the Cayley-Dickson construction, introducing pairs of non-zero hypercomplex vectors $A, B \in \mathbb{S}$ such that:

$$A \odot B = 0 \quad \text{where} \quad A \neq 0, B \neq 0$$

If we reverse the directionality of this algebraic operation—interpreting the equation from right to left—we discover the fundamental mechanism of topological genesis. It represents "nothing" (a null physical metric, a zero-energy vacuum state, or an unmanifested potential) destabilizing and factoring apart into two non-zero, complementary wholes (A and B).

The sedenion zero divisor acts mathematically as an agent of creation. It provides the precise algebraic language needed to model how unified, empty vacuum fields undergo spontaneous symmetry breaking to project distinct, paired physical structures into existence.

8.2. Hierarchical Scaling Laws of Life

Biological systems do not operate within a single isolated layer of physical reality; they exist as a deeply integrated cascade of nested hypercomplex spaces. The octonions analyzed in this paper are uniquely optimized for modeling the individual, discrete "building materials" of life.

These materials exist in two distinct, complementary functional domains:

Nucleic Acids (Information Space): Dealing in the storage, replication, and utilization of intangible, non-local genetic sequences.

Proteins (Operational Space): Executing the physical, localized mechanical work, enzymatic catalysis, and structural maintenance of the living system.

To model the continuous, sophisticated integration of these two distinct 8D octonionic spaces into a single, self-sustaining entity, the mathematics must expand. It requires the 16-dimensional sedenion framework to act as the overarching coordinator. The global sedenionic architecture governs a strictly nested geometric hierarchy:

$$\mathbb{S}^{16} \longrightarrow \mathbb{O}^{8} \longrightarrow \mathbb{H}^{4} \longrightarrow \mathbb{C}^{2} \longrightarrow \mathbb{R}^{1}$$

- Complex (2D Complex Wave-Particles): The foundational quantum units out of which all physical matter and gauge fields are constructed.
- Quaternions (4D Quaternionic Trajectories): The localized, relativistic classical spacetime coordinates that govern physical orientation, torque, and fluid configurations.
- Octonions (8D Octonionic Fields): The non-associative, history-dependent domains that isolate specific biological building materials (individual protein folding spaces and isolated nucleic acid code strings).
- Sedenions (16D Sedenionic Continuum): The fully integrated, living macroscopic organism, capable of utilizing zero-divisor projection operators to cross-modulate information space and operational space simultaneously.

9. Discussion

We have demonstrated—if not definitively proved—that advanced mathematics is fundamentally capable of capturing the underlying principles of living systems. The living of life involves the highly sophisticated, non-linear integration of countless disparate components into a fully functioning, unified macroscopic entity.

To contextualize this complexity, consider a comparison between a simple unicellular bacterium and a modern smartphone. An iPhone is remarkably sophisticated, managing

billions of discrete transistor states to execute diverse, high-level digital tasks. Yet, despite this technical prowess, it remains fundamentally inert; it cannot autonomously harvest mineral ores from the earth, refine raw petrochemicals into plastics, or assemble a duplicate of itself—much to the commercial distress of its manufacturers.

Conversely, if one places a single bacterium—or, on a macro-scale, a couple of teenagers—into almost any energetic environment, the underlying metabolic or behavioral algorithms will reliably yield two or more identical entities in short order. Life possesses an innate, self-referential generative capacity that entirely evades classical, linear mechanical descriptions. It is ultra-sophisticated, and it demands an equally ultra-sophisticated mathematical vocabulary to properly articulate, model, and analyze its behavior.

The dominant Victorian view of biology, genetics, and evolutionary theory posits that life is merely the serendipitous byproduct of a random series—a very long, highly numerous sequence—of entirely fortunate molecular accidents. However, a rigorous, structural study of biochemistry, metabolic cycles, coordinated protein folding, DNA replication mechanics, ribosomal translation, and the tight structural constraints of the Last Universal Common Ancestor (LUCA) reveals this accidental paradigm to be mathematically untenable.

Every practical experience of stochastic, unguided changes occurring within an intricate, high-dimensional system demonstrates that random perturbations invariably degrade systemic efficiency, driving the architecture toward decay rather than organization.

It is the sincere hope of the author that, by establishing these rigid hypercomplex frameworks, biology will ultimately transcend its current reliance on vague, qualitative descriptions and ambiguous linguistic metaphors. By joining physics and chemistry in the exact delights of rigorous "math-speak," biology can finally map the true, geometric blueprint of the living state.

Acknowledgments

The author expresses sincere gratitude to the independent research community and peer reviewers whose insightful feedback helped refine the scalar-body/vector-mind duality conceptual framework. Special thanks are due to those who provided computational validation and algebraic cross-checks for the quaternion torque calculations. This work did not receive any specific grant from funding agencies in the public, commercial, or not-for-profit sectors.

References

Lane, N. (2015). *The Vital Question: Energy, Evolution, and the Origins of Complex Life.* W. W. Norton & Company.

de Duve, C. (1995). *Vital Dust: Life as a Cosmic Imperative*. Basic Books.